IOP Conference Series: Materials Science and Engineering

PAPER • **OPEN ACCESS**

Fretting Biocorrosion Behaviour of Titanium-Zirconia composites in Foetal Bovine Serum

To cite this article: L Semetse *et al* 2019 *IOP Conf. Ser.: Mater. Sci. Eng.* **655** 012034

View the article online for updates and enhancements.

This content was downloaded from IP address 198.54.66.70 on 13/01/2020 at 07:21

IOP Conf. Series: Materials Science and Engineering **655** (2019) 012034 doi:10.1088/1757-899X/655/1/012034

Fretting Biocorrosion Behaviour of Titanium-Zirconia composites in Foetal Bovine Serum

L Semetse[1,*], B A Obadele[1], L Raganya[1,2], J Geringer[3] and P A Olubambi[1]

[1]Centre for Nanoengineering and Tribocorrosion, School of Mining, Metallurgy and Chemical Engineering, University of Johannesburg, Doornfontein Campus, Johannesburg, South Africa

[2]Light Metals, Materials Science & Manufacturing, Council for Scientific and Industrial Research, Meiring Naudé Road, Brummeria, Pretoria 0184, South Africa

[3]Univ Lyon, IMT Mines Saint-Etienne, Centre CIS, [STBio] Univ Jean Monnet, INSERM, SainBioSE, F-42023 Saint-Etienne France

E-mail: lerato.semetse@gmail.com

Abstract. This work aims at studying the fretting biocorrosion response of newly developed Ti-6Al-4V/ZrO_2 in simulated body fluid. Ti-6Al-4V alloy with different volume fractions of ZrO_2 produced via powder metallurgy techniques were spark plasma sintered to produce Ti-6Al-4V composites with improved properties. The microstructures of the resulting spark plasma sintered composites were examined using a scanning electron microscope (SEM). Fretting corrosion tests were conducted for each material composition with a special device used for fretting corrosion investigations with a cylinder-on-flat configuration. The tests were done in foetal bovine serum maintained at ambient temperature. Open circuit potential, dissipated energy and coefficient of friction were monitored throughout the experiments. The results show that the microstructures produced after zirconia additions were very different from those observed in pure Ti-6Al-4V. The presence of zirconia promoted the formation of globular zirconia-rich agglomerates throughout the matrix, leading to more improved fretting biocorrosion properties of Ti-6Al-4V.

1. Introduction

Metallic materials account for the widest application in biomedical devices (Jayaraj and Pius, 2018); however, the use of metals also poses some shortcomings and challenges due to their corrosion and degradation in the human body. Body fluids in contact with the implant device act as a corrosive media, which accelerates the degradation process in the presence of mechanical action such as walking, running or jumping (Sivakumar et al., 2018). Tribocorrosion processes result in accelerated material loss due to the combined effect of both wear and corrosion; leading to deterioration, poor performance and ultimate failure of the implant device (Mathew et al., 2009, Cruz et al., 2011). Tribocorrosion effects can thus translate to serious health implications, originating from the potential toxicity of degradation products like metal ions and wear debris when introduced into the human body (Bidhendi and Pouranvari, 2018, Zhang et al., 2018, Matusiewicz, 2014, Leopold et al., 2000).

Content from this work may be used under the terms of the Creative Commons Attribution 3.0 licence. Any further distribution of this work must maintain attribution to the author(s) and the title of the work, journal citation and DOI.
Published under licence by IOP Publishing Ltd

Austenitic stainless steels, titanium and titanium alloys as well as cobalt-chromium based alloys fall amongst the most common metallic biomaterials due to their excellent corrosion properties and acceptable biocompatibility (Anderson, 2001).
These metals owe their corrosion resistance to the stable oxide layer that forms on the surface, which shields them from most corrosive environments (Cruz et al., 2011). Load-bearing orthopaedic implants often fail due to the breakdown of this protective layer as a result of exposure to high loads and corrosive body fluids (Duisabeau et al., 2004). The breakdown of the oxide layer leads to generation of wear debris and corrosion particles. This interaction between electrochemical and mechanical effects promotes increased material loss (Mathew et al., 2009). Because of this, the goal with most biomaterials used for implants has been to develop materials with excellent biocompatibility and corrosion resistance as well as adequate mechanical properties for the intended function (Gilbert and Mali, 2012). The drawback with titanium and its alloys in load-bearing orthopaedic implant applications is the poor wear resistance (Mindivan, 2016, Obadele et al., 2015a).
Over the years, some attempts have been made into enhancing the properties of titanium by introducing various alloying elements such as Zr, Nb, Ta, and Mo to improve its mechanical and biocompatibility properties (Li et al., 2014, Hua et al., 2017). More recently, advanced manufacturing techniques have made it possible for a broad range of materials like composites, ceramics and new alloys to be investigated for biomedical applications (Bose et al., 2017, He et al., 2015, Buciumeanu et al., 2017, Karanjai et al., 2008). It has been observed that the introduction of inert ceramics like zirconia into the matrices of titanium-based materials through powder metallurgy techniques to produce metal matrix composites, is effective in improving the wear and tribocorrosion properties of titanium-based materials (Obadele et al., 2017). Obadele et al. (Obadele et al., 2015c) studied the wear behaviour of Ti-6Al-4V and composite coatings of laser cladded TiNi with different compositions of zirconia and reported that addition of zirconia produced a more refined microstructure and also led to a considerable improvement in the hardness and wear behaviour of the titanium composite.
This work aims to study the fretting corrosion behaviour of spark plasma sintered Ti6Al4V-ZrO_2 composites in simulated body fluid, for potential use in biomedical applications. The effect of zirconia content on the tribological properties of Ti6Al4V will be established.

2. Materials and method

The materials investigated were spark plasma sintered Ti-6Al-4V, Ti6Al4V+5%ZrO2 and Ti6Al4V+10%ZrO2. The Ti6Al4V and Ti6Al4V composites were cut to 9 × 9 × 15 mm parallelepipeds. Commercially available Ti-6Al-4V was used as the counter material from a forged process. The samples were ground down using 3 µm diamond suspension, thereafter polished with colloidal silica until a mirror surface was achieved. Afterward, the composites were washed with deionized water and dried with an automatic drier.
The fretting corrosion experiments were conducted on a special set-up device used for fretting corrosion investigations (see Figure 1). It is a derivative of the Tribomines® device that has been reported in fretting corrosion investigations by (Geringer et al., 2005, Kim and Geringer, 2012, Geringer et al., 2013). Similar experimental procedure was followed in this work. Linear voltage displacement transducer (LVDT) sensors on the device are in charge of controlling displacement, which exists within a range of ±10-100 µm. The flat and cylindrical samples were fixed onto the device's sample holders by means of insulated metallic screws. Fretting corrosion tests were conducted Foetal bovine serum (FBS), 30g/L of protein, Biowest®). Unlike other simulated body fluids which contain only inorganic species with compositions equal to those in human body fluids, FBS also contains proteins and organic molecules such as serum albumin; which have been found to have a significant effect on the corrosion and tribocorrosion behaviour of a material (Hang et al., 2010) (Geringer et al., 2013). The test was conducted at a frequency of 1 Hz. This was done to simulate the assumed average human gait as reported by Geringer et al., 2005. A normal load F_n of 85 N was used for each composite. A displacement of 0.08 mm sufficient to induce gross slip was imposed on the contact during testing. A relative displacement between the stem and bone of a hip implant is reported to be between 0.02-0.06 mm (Kim and Geringer, 2012). Fretting corrosion

experiments were carried out at room temperature and pressure. Each experiment was repeated three times for each composition. Due to the long test durations, and complex test set-up; room temperature was used to ensure reproducibility. Other studies with similar equipment and set-up have reported fretting corrosion tests for medical applications at room temperature (Geringer et al., 2013, Geringer et al., 2005, Kim et al., 2013). A three-electrode configuration was used in order to measure and control the electrochemical measurements of the metal couple; using a Parstat 2263 Potentiostat. A metallic wire was welded onto the sample, which served as the working electrode. For controlling and monitoring the potential, a platinum and saturated calomel electrode (SCE) served as the counter and reference electrodes respectively. Mechanical and electrochemical data acquisition software was employed to record data generated throughout the test such as friction coefficient, tangential force-displacement cycles (F_T – D cycles) and open circuit potential. After each test, the samples were removed from solution and rinsed with deionized water. The wear track area and contact zones were characterized using a non-contact three-dimensional optical profilometry and a scanning electron microscope.

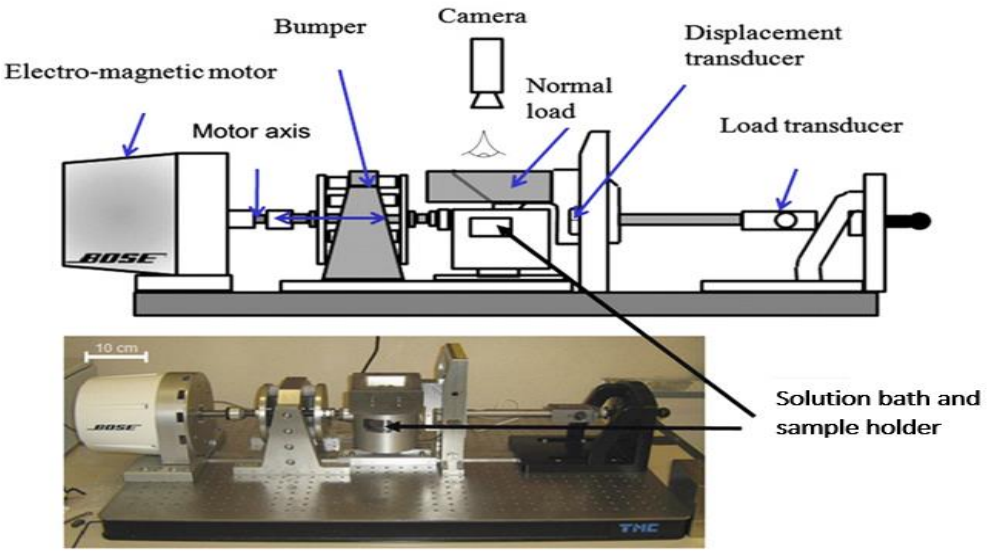

Figure 1: A schematic and image of the fretting corrosion test set-up used in the experiments; reported by (Kim et al., 2013).

3. Results and Discussion

3.1. Microstructural analysis of the as-received samples

The SEM micrographs of the sintered composites without and with ZrO_2 (Ti-Al-4V, Ti-Al-4V /+5/+10%ZrO_2) are shown in Figure 2. The microstructure of Ti-6Al-4V as shown in Figure 2(a) comprises a lamellae structure of alpha and beta (light) phases. The darker is alpha phase while the light is beta phase. This type of microstructures could be related to the alloy fabricated by Obadele et al. (Obadele, 2014, Obadele et al., 2017). This illustrates that unreinforced Ti-6Al-4V alloy sintered at temperatures of 1000 °C and above using spark plasma sintering method, produced a fully lamellae microstructure.

The microstructures shown in Figure 2(b) and (c) are visibly different from those of sintered Ti-6Al-4V (in Figure 2(a)). The presence of zirconia resulted in the formation of agglomerates which are rich in zirconia, as shown on the EDS spectra in Figure 2(d). The presence and amount of the zirconia-rich agglomerates is better illustrated by the smaller OM images taken at a low magnification of 10X. The microstructure of Ti-6Al-4V with 5% ZrO_2 presented a smaller distribution of the zirconia-rich agglomerates, together with some platelet phases. The agglomerates are fewer and not uniformly

distributed. Furthermore, the microstructure obtained for Ti-6Al-4V with 10% ZrO_2 showed a higher region rich in zirconia agglomerates within the matrix as a result of the amount of zirconia present in the matrix. In another study by Obadele et al., 2017, SEM micrographs showed flower-like microstructures where the light areas were the zirconia-rich phases.

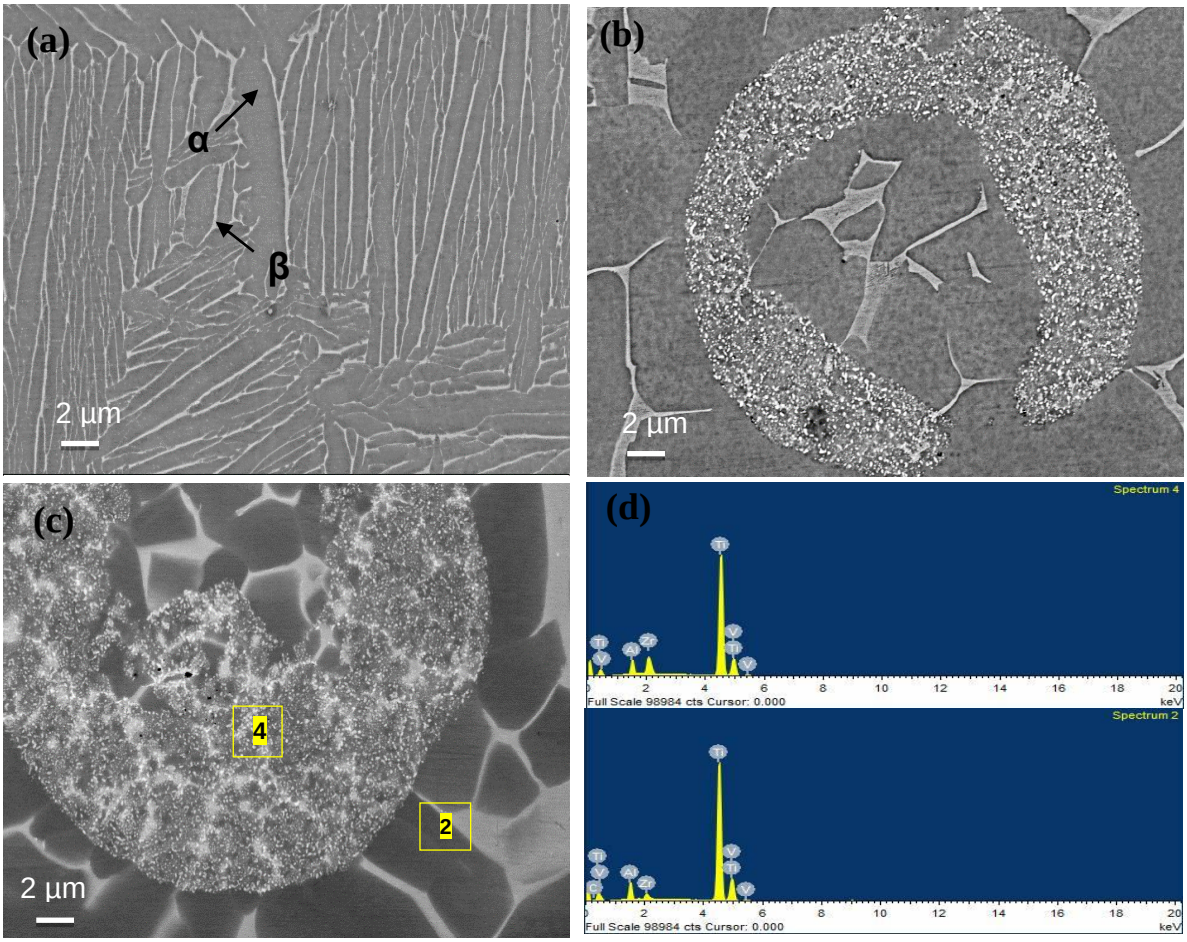

Figure 2. SEM micrographs of the as-received (a) Ti-6Al-4V, (b) Ti-6Al-4V+5%ZrO_2 and (c) Ti-6Al-4V+10%ZrO_2; (d) EDS

3.2. Open circuit potential before, during and after fretting Biocorrosion

The OCP evolution of Ti-6Al-4V without and with 5% and 10% ZrO_2 in foetal bovine serum (FBS) with no applied load and friction is given in Figure 3 (a). The most stable potential is displayed by Ti-6Al-4V with 5% ZrO_2 addition without applied load. The graph showing OCP evolution when fretting corrosion is taking place is given in Figure 3 (b). Generally, open circuit reading during fretting corrosion tests comprises three distinct zones, namely; the initial stabilization stage, fretting region and final stabilization stage. The OCP before, during and after fretting in FBS is presented in Figure 3 (b) for Ti-6Al-4V without and with 5% and 10% ZrO_2 under an applied load of 85 N respectively. It could be seen that stable potentials of -0.5, -0.2 and -0.2 V were recorded for Ti-6Al-4V, 5% and 10% ZrO_2 addition respectively before fretting. At the onset of fretting, there is a significant drop in corrosion potential towards the negative values. The OCP values obtained are -1.0 ±0.03, -0.7 ±0.03 and -0.8 ±0.03 V for Ti-6Al-4V with 5% and 10% ZrO_2 additions. Nevertheless, the highest OCP drop is obtained for sintered Ti-6Al-4V with Ti-6Al-4V counterface, suggesting a higher tendency to metallic dissolution under friction conditions in FBS. This could be due to disruption of the naturally

formed oxide layer exposing a fresh underlying metal surface to the electrochemical solutions (Gilbert and Mali, 2012). The low OCP values during fretting are an illustration of the electrochemical activity taking place between the underlying material and solution where the passive film has been destroyed.

The fluctuations observed during fretting indicate repassivation and depassivation, a phenomenon that results in continuous destruction and formation of the metal's surface oxide (McTighe et al., 2015). According to Ponthiaux et al. (Ponthiaux et al., 2004), the OCP recorded during fretting is usually a mixed potential emanating from the worn and unworn areas of the materials in contact, particularly in case whereby the material being tested and the counterface material are the same. When the OCP values of the sintered composites are compared with respect to the ZrO_2 content, Ti-6Al-4V with 10 wt.% ZrO_2 shows the lowest OCP decline, indicating the most stable passive film formation and high resistance to plastic deformation. In contrast, the composite having 5 wt.% ZrO_2 is showing less stability during the combined effect of wear and corrosion, as opposed to when there was no load applied. As a conclusion, the ZrO_2 content has an influence in improving the OCP behaviour. Increasing zirconia from 5 wt.% to 10 wt.% in Ti-6Al-4V increases the stability of the passive layer. This observation was reported by Obadele et al., 2015b, where TiNi+10%ZrO_2 were found to have better tribocorrosion response in acidic media compared to TiNi+5%ZrO_2 under similar conditions.

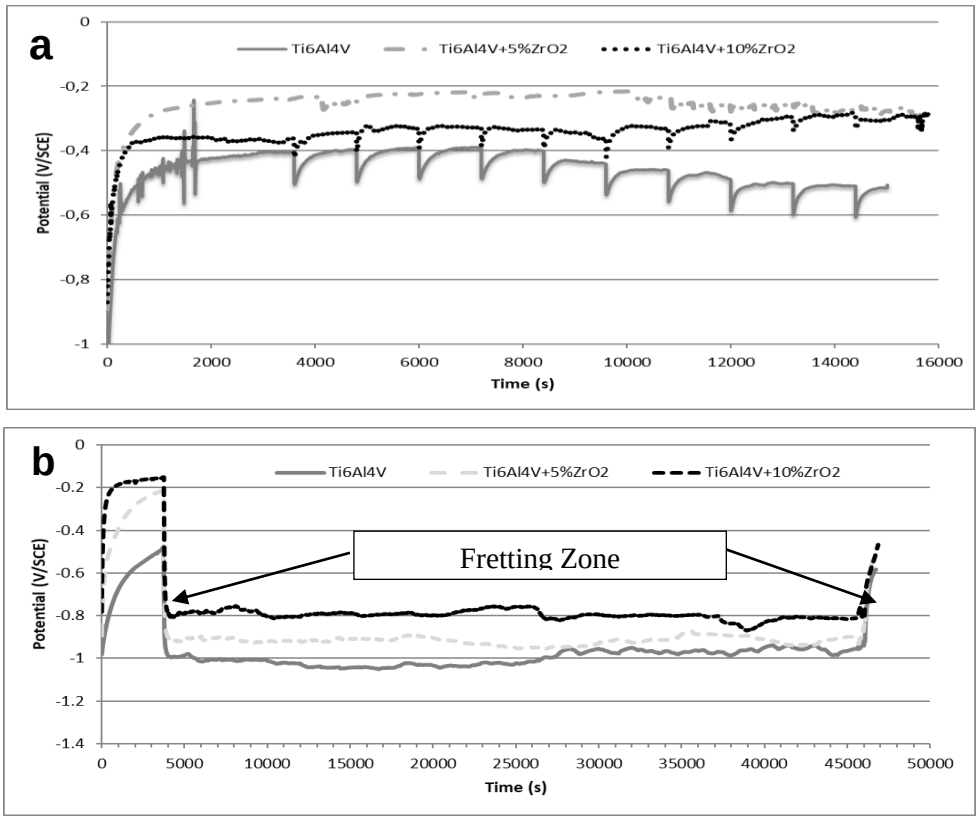

Figure 3. OCP evolution with (a) without an applied load and (b) at applied load of 85 N for Ti-6Al-4V, Ti-6Al-4V+5/+10% ZrO_2 sintered composites.

Generally, a decrease in the electrode potential of a material is indicative of an increased tendency of the material surface to corrosion (Mathew et al., 2011). Mischler stated that the measured potential during the fretting regime is a reflection of the galvanic coupling between the worn areas (underlying metal exposed to solution by destruction of the passive film) and unworn areas (passive metal) (Mischler, 2008). The open circuit potential therefore serves as a method to monitor the corrosion response of a material under different test conditions, and to assess the stability of the oxide film under such conditions. From comparison, Ti-6Al-4V with 10% ZrO_2 showed the best fretting corrosion stability due to the higher potential values maintained throughout the test duration. This could be as a result of higher ZrO_2 content

within the matrix of this material, which produced a refined microstructure with a high distribution of ZrO_2 rich agglomerates.

3.3. Fretting loops during biocorrosion

The fretting regimes in this study were obtained from the plots of tangential force versus displacement loops obtained during fretting corrosion experiments at 85 N, and these are given in Figure 4. It could be seen that the tests show a gross slip regime for all compositions. Additionally, the development of sharp peaks on the curve can be observed for Ti-6Al-4V with 5% ZrO_2 addition in Figure 4(b) and (c). This effect has been reported to occur due to the ploughing effect or the interlocking of geometric features in the contact surfaces. Flatter parallelogram shapes have been found to produce low coefficient of friction (COF) values (Tobi et al., 2017). Fretting mechanisms maps have demonstrated that low loads together with high displacements lead to gross slip conditions which is associated with wear, whereas high loads with low displacements promote partial slip conditions (Tobi et al., 2017). These observations are in agreement with the current study in terms of the resulting fretting loops, even though the experiments were conducted under the same displacement.

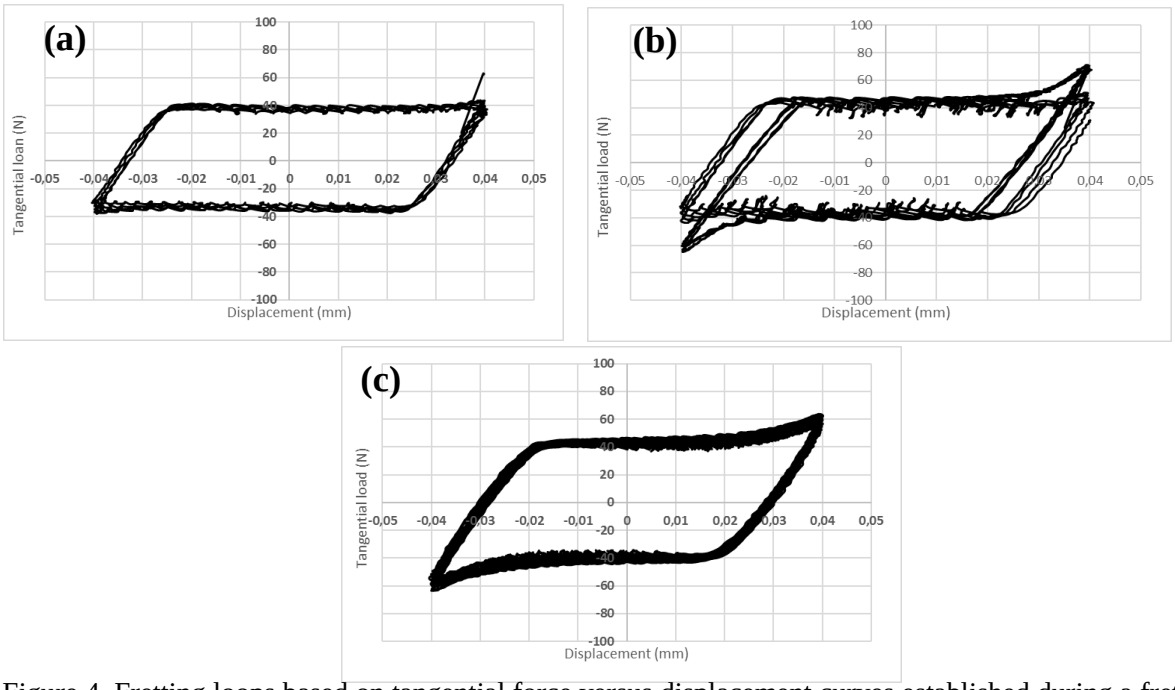

Figure 4. Fretting loops based on tangential force versus displacement curves established during a fretting corrosion tests for (a) Ti-6Al-4V, (b) Ti-6Al-4V+5% ZrO_2, and (c) Ti-6Al-4V+10% ZrO_2 at 85 N.

3.4. Friction coefficient during fretting

Friction coefficient evolution with time during fretting corrosion experiments for Ti-6Al-4V with 5 and 10% ZrO_2 are shown in Figure 5 at an applied load of 85 N and test duration of 16 h. Within the first few seconds of the test, the COF increases from about 0.4 and 0.6 to 0.8 and 0.9, where it stabilises for some time and decreases slightly towards the end of the experiment. The initial increase in COF at the beginning of the test is referred to as the running-in-period and has been reported in literature (Kim et al., 2013, Ding et al., 2018). Johnson (Johnson, 1995) defines the 'running-in' stage as the change in the surface profile that occurs on a smooth or rough surface during repeated sliding. During this running-in period, the COF increases due high friction resulting from surface asperities that may be present on the surfaces of contacting materials in the initial stages of fretting (Kim et al., 2013).

At around 20000 s and 35000 s in Figure 5(a) and 5(b), fluctuations could be observed for Ti-6Al-4V and 5% ZrO_2 respectively; it is also around this time where the curves tends to decrease slightly. This fluctuations could be as a result of hard ceramic particles of ZrO_2 that may be present on the surfaces of the fretting bodies (Obadele et al., 2015a). Mindivan (Mindivan, 2016) reported a similar behaviour where the fluctuations were attributed to the abrasive effect of the generated wear particles, originating from the ceramic counterface. After the initial running-in, and stabilization of COF, a decrease in COF values could be observed over time for all compositions, to values close to 0.4 at the end of the test. These observations correspond to results obtained by Geringer and Macdonald (Geringer and Macdonald, 2014) were it was observed that during fretting corrosion tests, the friction coefficient of a material couple decreased over time. That is, friction coefficient values were lower at the end of experiments which had a higher number of cycles. This behaviour was attributed to reduced friction due to smoother surfaces forming over long duration experiments. Looking at all OCP curves, it can be observed that there are less fluctuations for Ti-6Al-4V+10% ZrO_2 indicating the stability of this composition under friction.

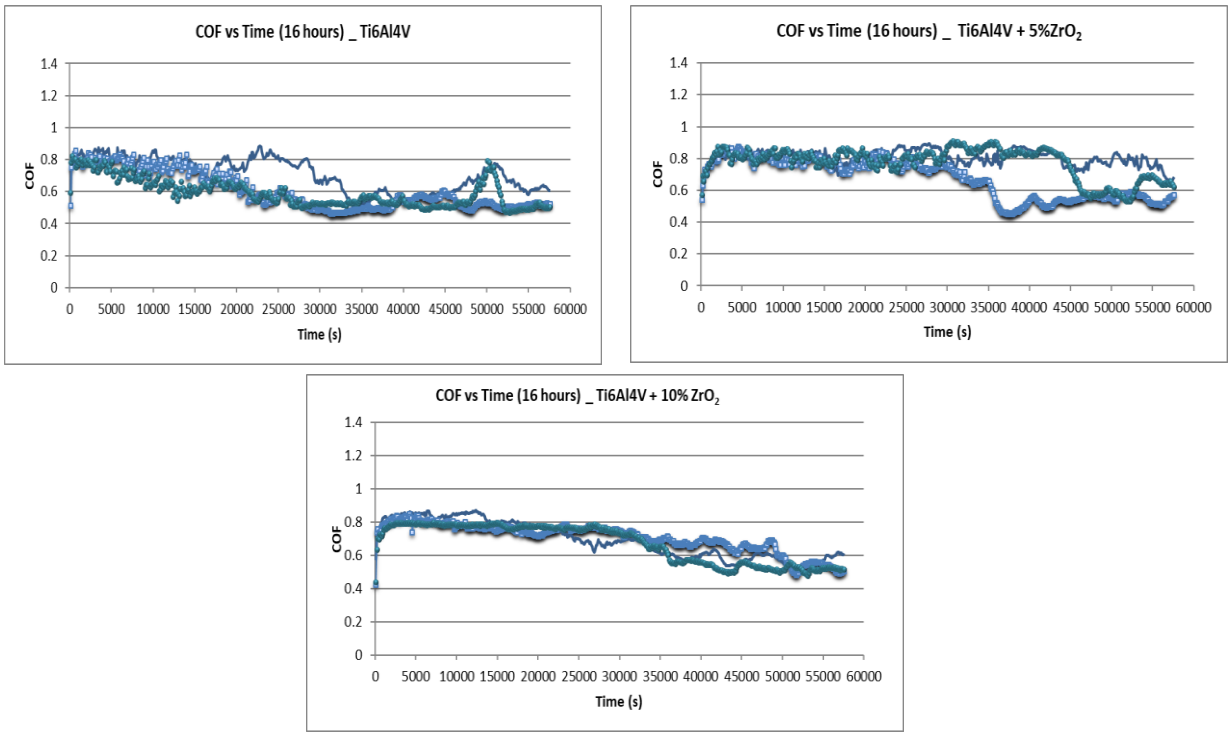

Figure 5. Friction coefficient for (a) Ti-6Al-4V, (b) Ti-6Al-4V+5% ZrO_2, and (c) Ti-6Al-4V+10% ZrO_2 under an applied load of 85 N.

4. Conclusion

The fretting corrosion behaviour of Ti-6Al-4V without and with 5 wt.% and 10 wt.% ZrO_2 were investigated in foetal bovine serum at an applied load of 85 N. Open circuit potential was measured before, during and after fretting and the corresponding friction coefficient was reported. The results obtained showed that higher amount of zirconia (10 wt.%) had a significant effect in improving the overall fretting biocorrosion behaviour of Ti-6Al-4V. This was attributed to the refined microstructure obtained, having uniformly distributed zirconia-rich agglomerates throughout the matrix. Ti-6Al-4V+ 10% ZrO_2 composite exhibited the best tribological properties and better corrosion resistance during fretting, indicating that a higher content of zirconia is more effective in improving the tribological and electrochemical properties of Ti-6Al-4V.

5. Acknowledgement

The authors acknowledge the Centre for Nanoengineering and Tribocorrosion at the University of Johannesburg and the National Research Foundation for financial support. Special thanks to École des Mines de Saint-Étienne in France and Centre Ingénierie et Santé (CIS) laboratory for the training and use of facilities for fretting corrosion experiments.

References

[1] ANDERSON, J. M. 2001. Biological responses to materials. *Annual review of materials research,* 31**,** 81-110.
[2] BIDHENDI, H. R. A. & POURANVARI, M. 2018. Corrosion study of metallic biomaterials in simulated body fluid. *Metallurgical and Materials Engineering.*
[3] BOSE, S., KE, D., SAHASRABUDHE, H. & BANDYOPADHYAY, A. 2017. Additive manufacturing of biomaterials. *Progress in Materials Science*.
[4] BUCIUMEANU, M., ARAUJO, A., CARVALHO, O., MIRANDA, G., SOUZA, J., SILVA, F. & HENRIQUES, B. 2017. Study of the tribocorrosion behaviour of Ti6Al4V–HA biocomposites. *Tribology International,* 107**,** 77-84.
[5] CRUZ, H., SOUZA, J., HENRIQUES, M. & ROCHA, L. 2011. Tribocorrosion and bio-tribocorrosion in the oral environment: the case of dental implants. *Biomedical tribology,* 1-33.
[6] DING, H., FRIDRICI, V., GERINGER, J., FONTAINE, J. & KAPSA, P. 2018. Influence of diamond-like carbon coatings and roughness on fretting behaviors of Ti–6Al–4V for neck adapter–femoral stem contact. *Wear,* 406**,** 53-67.
[7] DUISABEAU, L., COMBRADE, P. & FOREST, B. 2004. Environmental effect on fretting of metallic materials for orthopaedic implants. *Wear,* 256**,** 805-816.
[8] FERNÁNDEZ-GARCÍA, E., GUTIERREZ-GONZALEZ, C., FERNANDEZ, A., TORRECILLAS, R. & LÓPEZ-ESTEBAN, S. 2013. Processing and spark plasma sintering of zirconia/titanium cermets. *Ceramics International,* 39**,** 6931-6936.
[9] GERINGER, J., FOREST, B. & COMBRADE, P. 2005. Fretting-corrosion of materials used as orthopaedic implants. *Wear,* 259**,** 943-951.
[10] GERINGER, J. & MACDONALD, D. D. 2014. Friction/fretting-corrosion mechanisms: Current trends and outlooks for implants. *Materials Letters,* 134**,** 152-157.
[11] GERINGER, J., PELLIER, J., TAYLOR, M. L. & MACDONALD, D. D. 2013. Fretting corrosion with proteins: The role of organic coating on the synergistic mechanisms. *Thin solid films,* 528**,** 123-129.
[12] GILBERT, J. L. & MALI, S. A. 2012. Medical implant corrosion: electrochemistry at metallic biomaterial surfaces. *Degradation of implant materials.* New York: Springer.
[13] HANG, R., MA, S., JI, V. & CHU, P. K. 2010. Corrosion behavior of NiTi alloy in fetal bovine serum. *Electrochimica Acta,* 55**,** 5551-5560.
[14] HE, D., ZHENG, S., PU, J., ZHANG, G. & HU, L. 2015. Improving tribological properties of titanium alloys by combining laser surface texturing and diamond-like carbon film. *Tribology international,* 82**,** 20-27.
[15] HUA, N., CHEN, W., ZHANG, L., LI, G., LIAO, Z. & LIN, Y. 2017. Mechanical properties and bio-tribological behaviors of novel beta-Zr-type Zr-Al-Fe-Nb alloys for biomedical applications. *Materials Science and Engineering: A,* 76**,** 1154-1165.
[16] IVKOVIC, B., DJURDJANOVIC, M. & STAMENKOVIC, D. 2000. The influence of the contact surface roughness on the static friction coefficient. *Tribology in industry,* 22**,** 41-44.
[17] JAYARAJ, K. & PIUS, A. 2018. Biocompatible coatings for metallic biomaterials. *Fundamental Biomaterials: Metals.* Elsevier.
[18] JOHNSON, K. L. 1995. Contact mechanics and the wear of metals. *Wear,* 190**,** 162-170.
[19] KARANJAI, M., SUNDARESAN, R., MOHAN, T. R. R. & KASHYAP, B. P. 2008. Evaluation of growth of calcium phosphate ceramics on sintered Ti–Ca–P composites. *Materials Science and Engineering: C,* 28**,** 1401-1407.
[20] KIM, K. & GERINGER, J. 2012. Analysis of energy dissipation in fretting corrosion experiments with materials used as hip prosthesis. *Wear,* 296**,** 497-503.

[21] KIM, K., GERINGER, J., PELLIER, J. & MACDONALD, D. D. 2013. Fretting corrosion damage of total hip prosthesis: Friction coefficient and damage rate constant approach. *Tribology International,* 60**,** 10-18.
[22] LEOPOLD, S. S., BERGER, R. A., PATTERSON, L., SKIPOR, A. K., URBAN, R. M. & JACOBS, J. J. 2000. Serum titanium level for diagnosis of a failed, metal-backed patellar component. *The Journal of arthroplasty,* 15**,** 938-943.
[23] LI, Y., YANG, C., ZHAO, H., QU, S., LI, X. & LI, Y. 2014. New developments of Ti-based alloys for biomedical applications. *Materials,* 7**,** 1709-1800.
[24] MATHEW, M., SRINIVASA PAI, P., POURZAL, R., FISCHER, A. & WIMMER, M. 2009. Significance of tribocorrosion in biomedical applications: overview and current status. *Advances in tribology,* 2009.
[25] MATHEW, M. T., UTH, T., HALLAB, N. J., POURZAL, R., FISCHER, A. & WIMMER, M. 2011. Construction of a tribocorrosion test apparatus for the hip joint: Validation, test methodology and analysis. *Wear,* 271**,** 2651-2659.
[26] MATUSIEWICZ, H. 2014. Potential release of in vivo trace metals from metallic medical implants in the human body: from ions to nanoparticles–a systematic analytical review. *Acta biomaterialia,* 10**,** 2379-2403.
[27] MCTIGHE, T., BRAZIL, D., KEPPLER, L., KEGGI, J. & MCPHERSON, E. 2015. Metallic Modular Taper Junctions in Total Hip Arthroplasty. *Reconstructive Review,* 5.
[28] MINDIVAN 2016. Comparative Study of Tribocorrosion Properties of Some Bio-Based Materials
[29] in Simulated Artificial Saliva. *Machines, Technologies, Materials***,** 58-60.
[30] MISCHLER, S. 2008. Triboelectrochemical techniques and interpretation methods in tribocorrosion: A comparative evaluation. *Tribology International,* 41**,** 573-583.
[31] NACHANE, R. P., HUSSAIN, G. F. S. & IYER, K. R. 1998. Theory of stick-slip effect in friction.
[32] OBADELE, B., ANDREWS, A., OLUBAMBI, P., MATHEW, M. & PITYANA, S. 2015a. Tribocorrosion behaviour of laser cladded biomedical grade titanium alloy. *Materials and Corrosion,* 66**,** 1133-1139.
[33] OBADELE, B. A. 2014. Tribocorrosion mechanisms in laser deposited titanium-based smart composite coatings.
[34] OBADELE, B. A., ANDREWS, A., MATHEW, M. T., OLUBAMBI, P. A. & PITYANA, S. 2015b. Improving the tribocorrosion resistance of Ti6Al4V surface by laser surface cladding with TiNiZrO2 composite coating. *Applied Surface Science,* 345**,** 99-108.
[35] OBADELE, B. A., ANDREWS, A., OLUBAMBI, P. A., MATHEW, M. T. & PITYANA, S. 2015c. Effect of ZrO2 addition on the dry sliding wear behavior of laser clad Ti6Al4V alloy. *Wear,* 328–329**,** 295-300.
[36] OBADELE, B. A., IGE, O. O. & OLUBAMBI, P. A. 2017. Fabrication and characterization of titanium-nickel-zirconia matrix composites prepared by spark plasma sintering. *Journal of Alloys and Compounds,* 710**,** 825-830.
[37] PONTHIAUX, P., WENGER, F., DREES, D. & CELIS, J.-P. 2004. Electrochemical techniques for studying tribocorrosion processes. *Wear,* 256**,** 459-468.
[38] ROYHMAN, D., PATEL, M., RUNA, M., JACOBS, J., HALLAB, N., WIMMER, M. & MATHEW, M. 2015. Fretting-corrosion in hip implant modular junctions: new experimental set-up and initial outcome. *Tribology international,* 91**,** 235-245.
[39] SIVAKUMAR, B., PATHAK, L. C. & SINGH, R. 2018. Fretting corrosion response of boride coated titanium in Ringer's solution for bio-implant use: Elucidation of degradation mechanism. *Tribology International*.
[40] TOBI, A. M., SUN, W. & SHIPWAY, P. 2017. Evolution of plasticity-based wear damage in gross sliding fretting of a Ti-6Al-4V non-conforming contact. *Tribology International,* 113**,** 474-486.
[41] ZHANG, Y., XIU, P., JIA, Z., ZHANG, T., YIN, C., CHENG, Y., CAI, H., ZHANG, K., SONG, C. & LENG, H. 2018. Effect of vanadium released from micro-arc oxidized porous

Ti6Al4V on biocompatibility in orthopedic applications. *Colloids and Surfaces B: Biointerfaces*, 169**,** 366-374.